



# Periodic Solutions in Non-Homogeneous Hill Equation

A. Rodriguez\* and J. Collado

*Automatic Control Department, CINVESTAV-IPN,  
Av. IPN 2508, Zacatenco, Mexico City, 07360, Mexico.*

Received: December 15, 2017; Revised: January 13, 2020

**Abstract:** Properties of  $T$  and  $2T$  periodic solutions in the homogeneous Hill equation have been entirely determined, but there is hardly any information about the existence of periodic solutions with different period. In this work,  $kT$  periodic solutions in the Hill equation will be explicitly characterized, here  $k$  is a natural number. Moreover, it will be shown that those  $kT$  periodic solutions become unstable when the system is forced with a function having the same period (or an integer multiple of it) of any of those solutions. As a consequence, two types of instability will be presented for the first time on the Ince-Strutt diagram: the well-known parametric resonance and the linear resonance due to the forcing signal.

**Keywords:** *non-homogeneous Hill equation;  $kT$ -periodic solutions; linear and parametric resonance; Ince-Strutt diagram; Floquet multipliers.*

**Mathematics Subject Classification (2010):** 34C25, 11J20.

## 1 Introduction

### 1.1 Hill equation

The general class of homogeneous second order linear differential equations with real periodic coefficients can be characterized by the Hill equation (1), it describes dynamical systems with intrinsic periodicity and parametric behaviour such as the modulation of radio carrier waves, transverse vibrations of a tense elastic member, the stability of a periodic motion in a non-linear system (linearization in a neighbourhood of a periodic motion) and the focus and defocus of particle beams in particle accelerators. Also, this equation can be seen as a particular case of the Schrödinger equation with periodic potential.

---

\* Corresponding author: <mailto:arodriguezm@ctrl.cinvestav.mx>

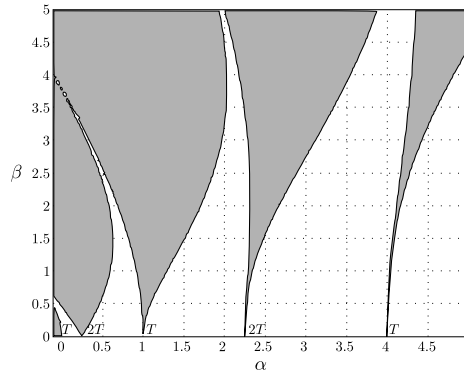


**Figure 1:** Stability-chart of the Mathieu equation:  $\ddot{x} + [\alpha + \beta \cos(t)] x = 0$ .

The Hill equation name arose after the transcendent publication ” of the memoir on the motion of the lunar perigee” by G. W. Hill [1], in which he established the mathematical foundations of the stability theory of parametric systems.

The Hill equation is denoted by

$$\ddot{x} + [\alpha + \beta f(t)]x = 0, \quad f(t) = f(t + T), \quad \int_0^T f(t)dt = 0, \quad (1)$$

where  $\alpha$  and  $\beta$  are two independent parameters.  $\sqrt{\alpha}$  is the natural frequency of the system of free oscillation in the absence of excitation,  $\beta$  is the amplitude of the parametric excitation (in most cases it is small).  $T > 0$  is the minimum period.

There are two particular forms of equation (1): the Mathieu equation [2]

$$\ddot{x} + [\alpha + \beta \cos(\omega t)]x = 0, \quad (2)$$

when the function  $f(t)$  is purely sinusoidal and the Meissner equation, in its simplest form:  $\ddot{x} + [\alpha + \beta \operatorname{sgn}(\cos(t))] x$ .

Stability of the solutions in the Hill equation can be seen in a two-parameter bifurcation chart known as the Ince-Strutt diagram [3], see Fig. 1. The white areas represent the values of parameters at which the solution is stable and the gray regions are the Arnold tongues or parametric resonance tongues [4], they depict unstable solutions.

Equation (2) admits at least one non-trivial periodic solution on the tongue boundaries. The tongues that born at  $\alpha = n^2, \beta = 0$ , for  $n = 1, 2, \dots$ , have one  $T$ -periodic solution, and the instability that occurs upon crossing such a tongue boundary is referred to as a harmonic instability. The other boundaries whose tongues arise at  $\alpha = (2n + 1)^2/4$  have one  $2T$ -periodic solution, see Fig. 1.

## 1.2 Parametric and linear resonance

Parametric resonance is a topic well studied and inherent to the homogeneous Hill equation. However, as we will see later, linear resonance can also be linked to the Hill type systems.

With a few exceptions, [5–8], the forced Hill equation has not been widely studied in the literature; in this work the  $kT$ -periodically forced system will be analysed, with  $k \in \mathbb{Z}_+ \setminus \{1, 2\}$ .

Parametric excitation of a system differs from direct forcing in that the fluctuations appear as a temporal modulation (usually periodic) of a parameter rather than as a direct additive term. The time dependence is explicit, which implies an external energy source and the possibility of unstable behaviour known as parametric resonance which is dependent upon the frequency of the parameter variation and the natural frequency of the system.

The rate of increase in amplitude of the response of a linear system with parametric resonance is exponential [9], whereas the typical resonance is characterized by a linear growth rate. Examples of parametric and linear resonance can be found in [10] and [11] respectively.

Through the Ince-Strutt diagram, only  $T$  or  $2T$ -periodic solutions appear, however the system (1) admits other  $kT$ -periodic solutions ( $k \in \mathbb{Z}_+ \setminus \{1, 2\}$ ), as it was specified in [12].

Such  $kT$ -periodic solutions come out as very slim lines on the stable zones in the stability diagram. The lines become unstable if the system (1) is forced by a periodic function containing at least one spectral line in its Fourier series with the same period as any of these  $kT$ -periodic lines, see Figures 5a and 5b. Further details will be provided in Section 3.

Even though, the existence of periodic solutions inside the stable regions was already known, the first one in obtaining (numerically) the values of parameters  $\alpha, \beta$  for which these periodic solutions arise was Jazar [13], he called them splitting lines. However, in this text they will be termed as *resonance lines* for the reasons that will be clear later.

It is important to highlight that before this work, the above-mentioned  $kT$ -periodic solutions were not studied in the context of stability for the Hill equation.

So far, we have only remarked the properties of the homogeneous Hill equation. Nevertheless, the study of the forced equation (3) also leads to interesting features.

$$\ddot{x} + \delta\dot{x} + [\alpha + \beta f(t)]x = g(t), \quad g(t) = g(t+T), \quad \int_0^T g(t)dt = 0, \quad (3)$$

Few studies have been developed around the non-homogeneous case, among them, one can find the results of Slane and Tragesser [8] who modified the Floquet theory so as to analytically examine the transitory and steady-state behaviour of a non-autonomous inhomogeneous system, but only for  $g(t+T) = g(t)$ . Younesian et al. [7] used the strained parameter technique to seek the asymptotic periodic solutions in the forced Mathieu equation, Shadman and Mehri [5] worked with fixed point theorems to investigate the existence of periodic solutions of the non-homogeneous Hill equation, Kwong and Wong [6] applied the Floquet theory to prove the conjecture that all solutions of a second order forced linear differential equation of Hill type are oscillatory on  $[0, \infty)$ . In addition, the damped forcing Hill equation can be obtained, after some light modifications, from the more general equation analyzed in [14].

Notice that in these previous contributions no damping effect was examined. Herein, the stability of a specific type of the non-homogeneous Hill equation with a linear dissipative term ( $\delta$ ) will be studied.

Finally, the results will be illustrated through the forced Kapitza pendulum which motivates the work. The behaviour of the pendulum is illustrated by numerical simulations for some specific values of  $\alpha, \beta$  and  $\delta$ .

## 2 Preliminaries

### 2.1 Floquet theory

A state-space representation of (1) is

$$\dot{x} = A(t)x \quad x \in \mathbb{R}^2 \quad \text{and} \quad A(t) = A(t + T) \in \mathbb{R}^{2 \times 2}, \tag{4}$$

where  $A(t)$  is a piecewise continuous matrix and  $T$  is the fundamental period.

For any initial condition, the general solutions of (4) can be written in terms of the state-transition matrix  $\Phi(t, t_0)$ , with  $\Phi(t_0, t_0) = I_2$ . Thus,

$$x(t) = \Phi(t, t_0)x(t_0). \tag{5}$$

The state-transition matrix evaluated at the end of a period,  $M = \Phi(T + t_0, t_0)$ , is known as *monodromy matrix*. Its eigenvalues, known as the *Floquet multipliers* or *characteristic multipliers*, determine the stability of the system (1), see [12] and [15]. They are independent of  $t_0$  [16], then it is possible and convenient to write  $M = \Phi(T, 0)$ .

**Theorem 2.1 ( Floquet [15] )** *The state-transition matrix  $\Phi(t, t_0)$  of the system (4) can be written as the product of two  $n \times n$ -matrices,*

$$\Phi(t, 0) = P(t)e^{Rt}, \tag{6}$$

where  $P(t)$  is a  $T$ -periodic  $n \times n$ -matrix function and  $R = \ln[\Phi(T)]/T$  is a constant  $n \times n$ -matrix, not necessarily real [17].

Any solution  $x(t)$  of (4) can be expressed as  $x(t) = \Phi(t, 0)x(0)$ . Then, for all  $t \geq 0$ ,  $t = kT + \tau$ ,  $k \in \mathbb{Z}_+ \triangleq \{m \in \mathbb{Z} : m \geq 0\}$  and  $\tau \in [0, T)$ ,

$$\begin{aligned} x(t) &= \Phi(kT + \tau, kT)\Phi(kT, (k - 1)T) \cdot \Phi((k - 1)T, (k - 2)T) \dots \Phi(T, 0)x(0) \\ &= \Phi(kT + \tau, kT)M^kx(0), \end{aligned} \tag{7}$$

it follows that the boundedness of  $\|x(t)\|$  depends exclusively on the boundedness of  $M^k$ .

In other words, let  $x(0)$  be the bounded initial conditions and  $\sigma(M) = \{\lambda_1, \lambda_2, \dots, \lambda_n\}$  are the spectrum of  $M$  (the set of all its eigenvalues), then

1.  $x(t) \rightarrow 0 \Leftrightarrow \sigma(M) \subset \overset{\circ}{D}_1 \triangleq \{z \in \mathbb{C} : |z| < 1\}$ .
2.  $x(t)$  is bounded  $\Leftrightarrow \sigma(M) \subset \bar{D}_1$  and  $\forall \lambda \in \partial D_1$  being simple roots of the minimal polynomial of  $M$ .  $\partial D_1$  is the boundary of the set  $D_1$ .
3.  $x(t) \rightarrow \infty \Leftrightarrow \exists \lambda \in \sigma(M) : |\lambda| > 1$  or  $\sigma(M) \subset \bar{D}_1$  &  $\exists |\lambda| = 1$ : is a multiple root of the minimal polynomial of  $M$ .

An equivalent stability analysis can be carried out using the eigenvalues of matrix  $R$  in (6) known as the *Floquet characteristic exponents* and defined by  $\mu = \ln(\lambda)/T$ . In this version the position of the eigenvalues about the imaginary axis is examined. The imaginary parts of the characteristic exponents are not determined uniquely, we can add  $2\pi i/T$  to each of them [15]. Nevertheless, the real part is unique.

## 2.2 Symplectic and $\varepsilon$ -symplectic matrices

**Definition 2.1** ([18]) The matrix  $Q \in \mathbb{R}^{2n \times 2n}$ ,  $n \in \mathbb{N}$ , is said to be symplectic if

$$Q^\top J Q = J, \quad J \triangleq \begin{bmatrix} \mathbf{0} & I_n \\ -I_n & \mathbf{0} \end{bmatrix}, \quad J^\top = -J = J^{-1}. \quad (8)$$

**Theorem 2.2** Let  $Q \in \mathbb{R}^{2n \times 2n}$  be a symplectic matrix, then it follows that

$$\lambda \in \sigma(Q) \Rightarrow \frac{1}{\lambda} \in \sigma(Q) \quad \text{and} \quad \bar{\lambda} \in \sigma(Q) \Rightarrow \frac{1}{\bar{\lambda}} \in \sigma(Q). \quad (9)$$

In words, the eigenvalues of  $Q$  are symmetric with respect to the unit circle.

**Lemma 2.1** A matrix  $Q \in \mathbb{R}^{2 \times 2}$  is symplectic if and only if its determinant is 1.

**Definition 2.2** A matrix  $Q \in \mathbb{R}^{2n \times 2n}$  is called symplectic with a multiplier  $\varepsilon$  (or  $\varepsilon$ -symplectic) if

$$Q^\top J Q = \varepsilon J, \quad \varepsilon > 0. \quad (10)$$

**Lemma 2.2** For  $\varepsilon > 0$ ,  $Q \in \mathbb{R}^{2n \times 2n}$  is  $\varepsilon$ -symplectic if and only if  $\det[Q] = \varepsilon$ .

The eigenvalues of a  $\varepsilon$ -symplectic matrix  $Q \in \mathbb{R}^{2n \times 2n}$  are symmetric with respect to the circle of radius  $\sqrt[2n]{\varepsilon}$ .

## 3 Stability Analysis

### 3.1 Unstable periodic solutions in the non-homogeneous Hill equation

According to the Floquet theory, the state-transition matrix satisfies  $\Phi(t + T) = \Phi(t)\Phi(T)$ . Therefore, for every solution  $x(t)$  of (1) with the initial condition  $x(0) = v$  ( $v$  is an eigenvector of  $\Phi(T)$  associated to  $\lambda$ ), the relation  $x(t + T) = \lambda x(t)$  holds. By iteration

$$\begin{aligned} x(t + T) &= \lambda x(t), \\ x(t + 2T) &= \lambda^2 x(t), \\ &\vdots \\ x(t + kT) &= \lambda^k x(t). \end{aligned} \quad (11)$$

It is easy to see that the  $kT$ -periodic solutions are obtained when  $\lambda^k = 1$ .

Then, from the last element of (11) and using the Euler formula,

$$x(t + kT) = \lambda^k x(t) = r^k e^{jk\theta} x(t). \quad (12)$$

Recalling that there are coordinates in which the Hill equation is Hamiltonian [15] and the state-transition matrix of a linear Hamiltonian system is symplectic [18], it follows that  $r^k = 1$  provided that  $\lambda^k \equiv 1$  for any  $k \in \mathbb{N}$ .

Then  $|e^{jk\theta}| = |\cos(k\theta) + j \sin(k\theta)| = 1$  and it is true when  $k\theta = \pm 2n\pi$  ( $n \in \mathbb{Z}$ ), hence

$$\theta = \pm \frac{2\pi}{k}, \quad (13)$$

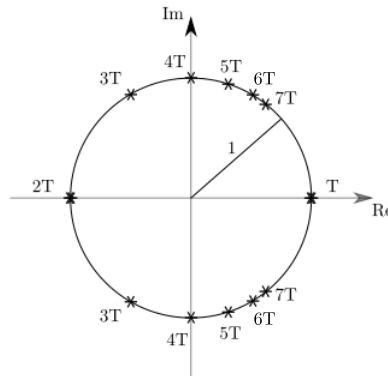


**Figure 2:** The unit circle shows the eigenvalues’ positions for several  $kT$ -periodic solutions corresponding to the curves shown on the Ince-Strutt diagram of the forced Mathieu equation.

$n$  is neglected because it only represents full rotations, i.e. spins of  $2\pi$  radians. *The angle condition* (13) determines for certain values of  $\alpha$  and  $\beta$ , the  $kT$ -periodic solutions (see Fig. 2). Thereby, the values of  $\lambda$  associated to the  $kT$ -periodic solutions are concluded as follows

$$\begin{aligned}
 k = 1, \theta = 2\pi &\Rightarrow \lambda_{1,2} = \{1, 1\}, \\
 k = 2, \theta = \pi &\Rightarrow \lambda_{1,2} = \{-1, -1\}, \\
 k = 3, \theta = \frac{2\pi}{3} &\Rightarrow \lambda_{1,2} = \left\{ -\frac{1}{2} \pm j \frac{\sqrt{3}}{2}, \right\}, \\
 k = 4, \theta = \frac{\pi}{2} &\Rightarrow \lambda_{1,2} = \{j, -j\}. \\
 &\vdots
 \end{aligned}$$

**Remark 3.1** As  $k$  is increased, the  $kT$ -periodic solutions come close to the  $T$ -periodic solutions. This can be appreciated principally in Fig. 2, but also in Fig. 5.

Now, consider the non-homogeneous Mathieu equation

$$\ddot{x} + [\alpha + \beta \cos(\omega_0 t)] x = \sum_{i=1}^r \gamma_i \cos(\omega_i t), \quad \omega_i = 2\pi/T_i, \tag{14}$$

$T_i = 2\pi/\omega_i$ ,  $T_0 \triangleq T$  and  $\omega_i$  are the frequencies of the forcing component.

The systems represented by (14) exhibit typical resonance in the same sense as the linear constant parameter systems.

**Proposition 3.1** *Linear resonance in the system (14) will arise when any forcing term in the summation satisfies  $T_i = k_i T_0$  for some  $k_i \in \mathbb{Z}_+$ .*

The condition (13) and the relation  $k_i = \omega_0/\omega_i$  allow to deduce

$$\theta_i = 2\pi \frac{\omega_i}{\omega_0}, \quad (15)$$

which establishes the  $T_i$ -periodic curves for the non-homogeneous system.

Two very important considerations arise from the previous analysis. First, the non-homogeneous Hill equation has two sources of instability: a) the parametric resonance which arises regardless of whether or not there is an input, and b) the linear resonance that appears when condition (15) is satisfied and, the parameters  $(\alpha_0, \beta_0)$  must be such that they generate solutions of period  $T_i$ . Secondly, for every system, equivalently for every stable point  $(\alpha, \beta)$  on the Ince-Strutt diagram, there is *only one* frequency for the system to come into resonance.

Notice that the parametric resonance appears when the system is evaluated at some coordinate  $(\alpha, \beta)$  on the dark regions of the stability diagram. The growth rate of the response of a system that undergoes parametric resonance is exponential unlike the linear resonance.

If the forcing signal has a  $T_0$ -periodic term, the boundaries corresponding to the  $T$ -periodic Arnold tongues become unstable [8]. Similarly,  $2T_0$ -periodic terms make the boundaries of the  $2T$ -periodic Arnold tongues unstable.

### 3.2 Non-homogeneous Mathieu equation with damping term

In this section, the dissipative effect on the inhomogeneous Mathieu equation is evaluated.

Consider the forced Mathieu equation and its state-space representation

$$\ddot{x} + \delta \dot{x} + [\alpha + \beta \cos(\omega_0 t)] x = \sum_{i=1}^r \gamma_i \cos(\omega_i t), \quad \delta > 0, \quad (16)$$

$$\begin{bmatrix} \dot{x}_1 \\ \dot{x}_2 \end{bmatrix} = \begin{bmatrix} 0 & 1 \\ -[\alpha + \beta \cos(t)] & -\delta \end{bmatrix} \begin{bmatrix} x_1 \\ x_2 \end{bmatrix} + \begin{bmatrix} 0 \\ 1 \end{bmatrix} \sum_{i=1}^r \gamma_i \cos(\omega_i t). \quad (17)$$

The results achieved in [8] suggest that the behaviour of the non-homogeneous Mathieu equation is practically the same as the homogeneous version, except when the characteristic multipliers equal to 1 are simple roots of the minimal polynomial of  $M$ . This justifies that the analysis is focused on system

$$\dot{x}_h = A(t)x_h, \quad A(t) = \begin{bmatrix} 0 & 1 \\ -\alpha - \beta \cos(t) & -\delta \end{bmatrix} \quad (18)$$

whose monodromy matrix is

$$M = M(T) = \begin{bmatrix} X_{1h}(T) & X_{2h}(T) \\ \dot{X}_{1h}(T) & \dot{X}_{2h}(T) \end{bmatrix}, \quad M(0) = \begin{bmatrix} 1 & 0 \\ 0 & 1 \end{bmatrix}. \quad (19)$$

Using the *Jacobi-Liouville* formula [15],  $\det[M(T)] = \det[M(0)]e^{\int_0^T \text{tr}[A(u)]du}$ , we get

$$\det[M(T)] = e^{-\delta T} < 1, \quad \delta > 0,$$

since  $\det[M(0)] = 1$  and  $\text{tr}[A(t)] = -\delta$ .

To estimate the Floquet multipliers and determine the stability of (18) we compute  $P_M(\lambda) = \lambda^2 - \text{tr}(M)\lambda + \det[M] = \lambda^2 - [X_{1h}(T) + \dot{X}_{2h}(T)]\lambda + e^{-\delta T}$ , the characteristic polynomial of  $M$ .

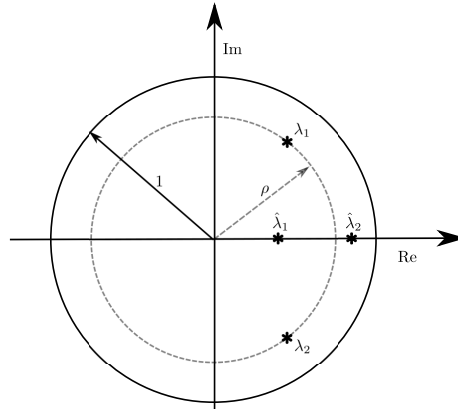


**Figure 3:** Eigenvalues of the  $\rho^1$ -monodromy matrix on the circle of radius  $\rho$  (inside the unitary circle), when they are complex  $\{\lambda_1, \lambda_2\}$  or on real-axis when they are real  $\{\bar{\lambda}_1, \bar{\lambda}_2\}$ .

**Proposition 3.2** *Let  $0 < \rho < 1$ , then the monodromy matrix  $M \in \mathbb{R}^{2 \times 2}$  is  $\rho^2$ -symplectic  $\Leftrightarrow \det[M] = \rho^2$ .*

**Remark 3.2** All the complex eigenvalues of  $M \in \mathbb{R}^{2 \times 2}$  are on the circle of radius  $\rho$ .

**Proof.** If  $\lambda_1 \in \mathbb{C} \Rightarrow \lambda_2 = \bar{\lambda}_1$ , thus  $\lambda_1 \bar{\lambda}_1 = \|\lambda_1\|^2 = \rho^2 \Rightarrow \|\lambda_1\| = \rho$ .

From previous analysis and Fig. 3, we can see that the characteristic multipliers  $\{\lambda_1, \lambda_2\} \in \mathbb{C}$  (on the  $\rho$ -radius circle) and the pair  $\{\bar{\lambda}_1, \bar{\lambda}_2\} \in \mathbb{C}$  (on real axis) are within the stable region, i.e., inside the unit circle.

The Arnold tongues of the direct forced Mathieu equation affected by distinct damping coefficients are displayed in Fig. 7. Notice that the resonance lines disappeared, this is owing to the Floquet multipliers that were on the unitary circle in Fig. 2 (which caused the resonance) were translated to the circle of radius  $\rho$  in Fig. 3. That is, the damping effect causes the characteristic multipliers move from the boundary of the unit circle to the circle with radius  $\rho$ .

The damping effect reduces the Arnold tongues by an order of  $1/e^{-\delta T}$ , see Fig. 7.

#### 4 The Kapitza Pendulum

The Kapitza pendulum is an inverted pendulum whose suspension point is changed periodically in the vertical direction. The objective from the point of view of control theory is the dynamic stabilization of the inverted position, usually when the suspension point is constrained to vibrate with a high frequency along the vertical axis. Its name is due to Pjotr Kapitza who explained in detail the particular behaviour of the system [19].

##### 4.1 General equation of the Kapitza pendulum

Fig. 4 shows a simple diagram of the inverted pendulum, where  $l$  is the length of a massless rigid rod with a small bob of mass  $m$  at the end,  $g$  is the gravitational constant,  $q(t)$  is the harmonic excitation function and  $(x, y)$  are the coordinates of the system.



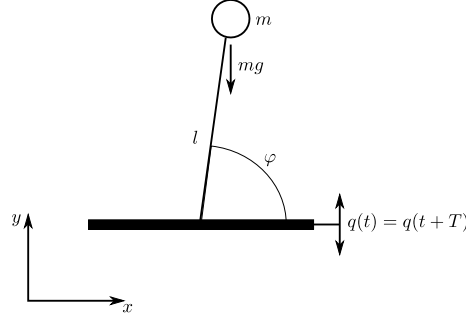


Figure 4: The Kapitza pendulum.

From Fig. 4, it can be deduced that

$$x = l \cos(\varphi), \quad \dot{x} = -l \sin(\varphi) \dot{\varphi}; \quad y = l \sin(\varphi) - q, \quad \dot{y} = l \cos(\varphi) \dot{\varphi} - \dot{q}.$$

Recalling the kinetic and potential energy:  $K = 1/2m(\dot{x}^2 + \dot{y}^2)$ ,  $U = mgl(l \sin(\varphi) - p)$ , applying the Euler-Lagrange equation  $d/dt \cdot \partial L / \partial \dot{\varphi} - \partial L / \partial \varphi = 0$ , where  $L = K - U$ . Linearizing the system around the upper equilibrium position, we obtain

$$\ddot{\varphi} + (-g/l + \ddot{q}/l) \varphi = 0.$$

This is the general equation of motion. However, it is useful to make some variable changes in order to recover the system (1). Hence, the Hill equation describes the Kapitza pendulum linearized around its upper equilibrium position.

## 4.2 Numerical results of the forced Kapitza pendulum

Since the Hill equation features the inverted pendulum, the system (3) describes its corresponding forced case.

The expressions

$$\ddot{x} + \delta \dot{x} + [\alpha + \beta \cos(t)] x = \sum_{k \in \{3, 5, 9, 14\}} \cos(t/k), \quad (20)$$

$$\ddot{x} + \delta \dot{x} + [\alpha + \beta \operatorname{sgn}(\sin(t))] x = \sum_{k \in \{3, 5, 9, 14\}} \cos(t/k), \quad (21)$$

are tested to investigate the dynamics of the Kapitza pendulum.

Figures 5a and 5b show the stability diagram for the forced pendulum represented by systems (20) and (21), respectively. The  $kT$ -periodic solutions in the homogeneous system being forced by any  $kT$ -periodic external function become unstable leading to the resonance lines represented by very slim dashed curves in Figures 5a and 5b. Each line has a corresponding pair of eigenvalues on the unit circle, see Figure 2.

Fig. 6a exhibits the periodic behaviour of the homogeneous Kapitza pendulum at the point  $(\alpha, \beta) = (3, 2)$  on the Ince-Strutt diagram, notice that this point is intercepted by a  $3T$ -periodic solution. Whereas Figures 6b and 6c show the response of the forced system, with the same  $(\alpha, \beta)$ -coordinates. The first graph illustrates the linear resonance

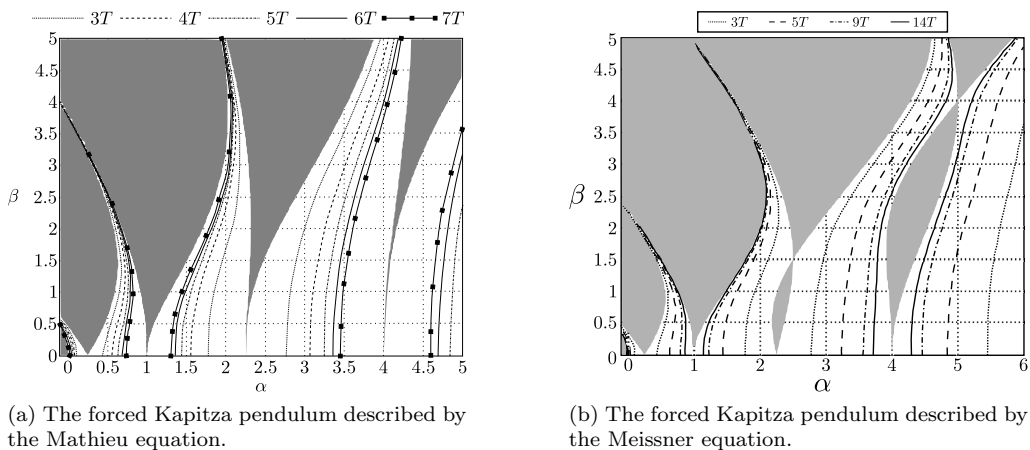


**Figure 5:** The Ince-Strutt diagrams of: (a)  $\ddot{x} + \delta\dot{x} + [\alpha + \beta \cos(t)]x = \sum_{k=3}^7 \cos(t/k)$  and (b)  $\ddot{x} + \delta\dot{x} + [\alpha + \beta \operatorname{sgn}(\sin t)]x = \sum_{k \in \{3,5,9,14\}} \cos(t/k)$ ,  $\delta = 0$ .

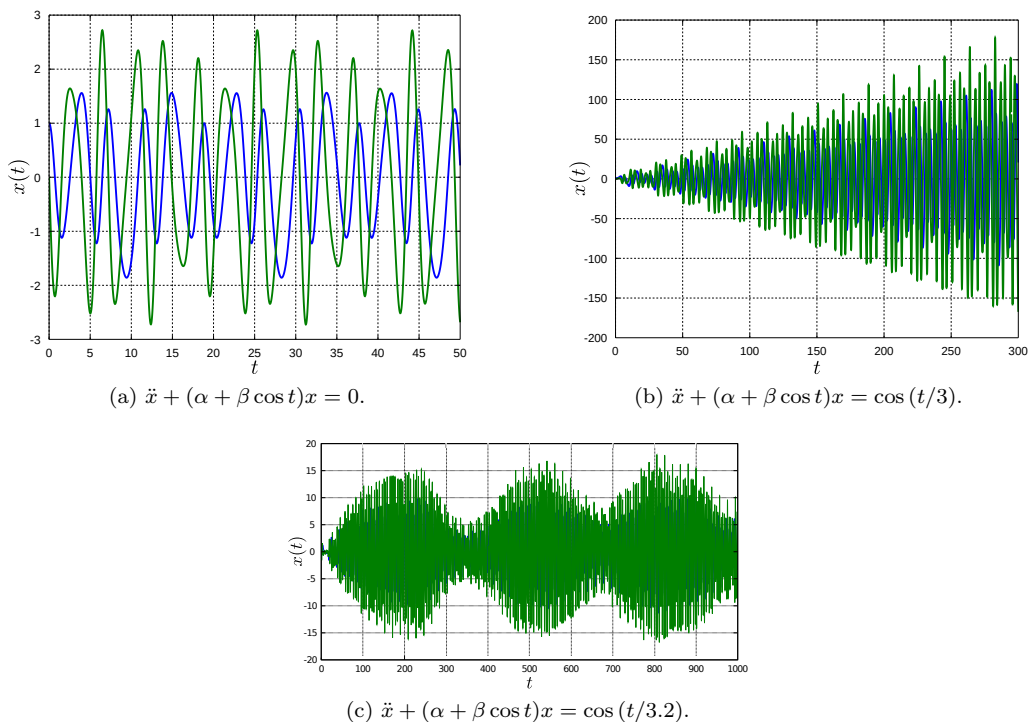


**Figure 6:** Response of the Kapitza pendulum: (a) homogeneous system,  $\alpha$  and  $\beta$  belong to a  $3T$ -periodic solution, (b) non-homogeneous system, the forced term is  $3T$ -periodic, hence linear resonance arises and (c) non-homogeneous system, the forced term is  $3.2T$ -periodic, in this case there can be no resonance.  $\alpha = 3$ ,  $\beta = 2$  in all the cases.

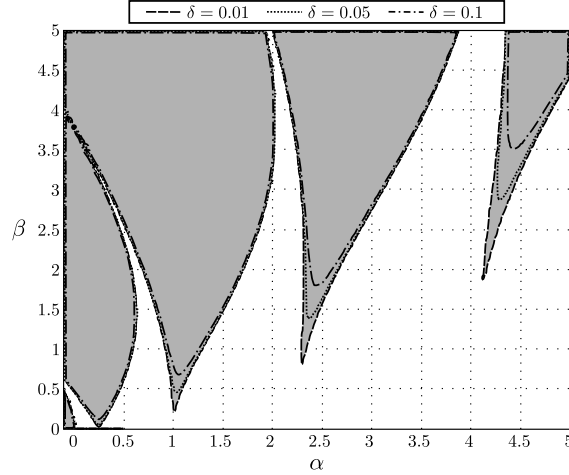


**Figure 7:** Stability diagram of the forced Kapitza pendulum:  $\ddot{x} + \delta\dot{x} + [\alpha + \beta \cos(t)]x = \sum_{i=3}^7 \cos(t/i)$  for different values of damping.

which arises due to the coincidence of the  $3T$ -periodic solution (in the non-homogeneous system) and the forcing signal (cosine) with the same period. In the second graph we see that the coincidence between the periods is lost (because the period of the cosine is  $T = 3.2$ ), consequently, the linear instability disappears.

Damping effect plays an essential role in the stability of the inverted pendulum, this reduces the area of parametric resonance in relation to the  $\delta$ -value (the greater dissipation means the less area of parametric instability). Regarding the linear resonance, it vanishes even with a relatively small value of dissipation, hence, the resonance lines disappear from the stability diagram, see Fig. 7. This fact is a direct consequence of Remark 3.2.

**Remark 4.1** A diagram similar to that of Fig. 5a for the forced Mathieu equation (20), for  $\alpha \in [-0.8, 0.6]$  and  $\beta \in [0, 1.5]$ , was obtained in [20], but no analysis was shown.

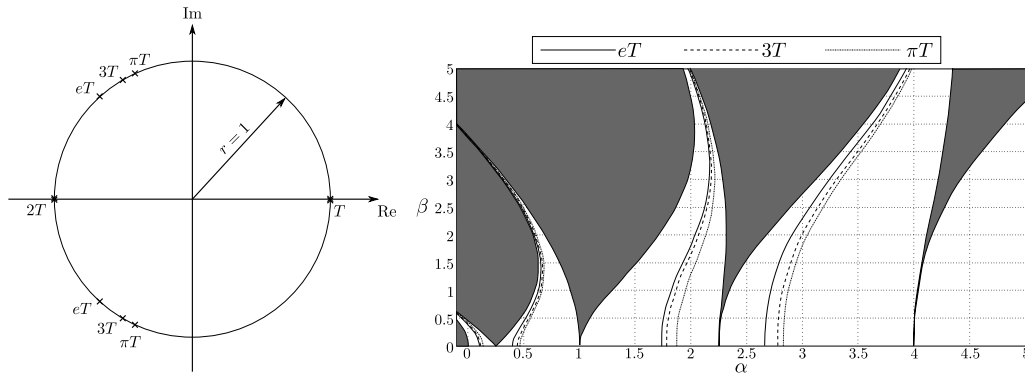
## 5 Further Results

In this section, we will analyze the system  $\ddot{x} + [\alpha + \beta f(t)]x = g(t)$ , where  $f(t) = f(t+T)$  and  $g(t) = g(t+\mathcal{T})$  with  $T$  and  $\mathcal{T}$  non-commensurable. More specifically, we will evaluate

$$\ddot{x} + [\alpha + \beta \cos(t)]x = \sin(\pi t), \quad \mathcal{T}_1 = 2, \quad (22)$$

$$\ddot{x} + [\alpha + \beta \cos(t)]x = \sin(et), \quad \mathcal{T}_2 = 2\pi/e, \quad (23)$$

where  $e \approx 2,7182818$  is the Euler number and  $\pi \approx 3.1415926$ , both are irrational numbers, and  $\mathcal{T}_1$  and  $\mathcal{T}_2$  are the fundamental periods of the forcing signals in (22) and (23) respectively. Since the minimal period of the parametric excitation term is  $T = 2\pi$ , it can be seen in a straight way that neither  $T$  and  $\mathcal{T}_1$  nor  $T$  and  $\mathcal{T}_2$  are commensurable.



(a) Positions of the eigenvalues for  $eT$ ,  $3T$  and  $\pi T$ -periodic solutions of the homogeneous Kapitza pendulum. (b) Resonance lines generated by the external signals:  $\sin(et)$ ,  $\sin(3t)$ ,  $\sin(\pi t)$ .

**Figure 8:** (a) Multipliers on the unitary disk representing  $eT$ ,  $3T$  and  $\pi T$ -periodic solutions of the homogeneous Kapitza pendulum. (b) stability diagram of the inverted pendulum forced with signals whose period is not commensurable with the parametric excitation term.

Use the condition  $\theta = 2\pi/k$  to obtain  $\pi$  and  $e$ -periodic solutions

$$\begin{aligned}
 k = \pi, \theta = \frac{2\pi}{\pi} &\Rightarrow \lambda_{1,2} \approx \{-0.4161 \pm j0.9092\}, \\
 k = e, \theta = \frac{2\pi}{e} &\Rightarrow \lambda_{1,2} \approx \{-0.6747 \pm j0.7380\}.
 \end{aligned}$$

Fig. 8a shows the Floquet multipliers positions associated with  $\pi T$ ,  $3T$  and  $eT$ -periodic signals. The multipliers of  $3T$ -periodic signals are plotted as a reference.

Notice that the behavior referring to the periodic solutions (in the homogeneous Hill equation) or the linear resonance (in the non-homogeneous Hill equation) is preserved in spite of the forcing signals and the parametric excitations are incommensurable, i.e., the  $kT$ -periodic solutions can appear with  $k$  not necessary integer provided that the eigenvalues of the monodromy matrix are on the unit circle. These solutions will resonate if a forcing term, with the same (or multiple) period, is applied to the system.

Fig. 9 traces the trajectories  $x(t)$  of the solutions of (22) when  $\alpha = 2$  and  $\beta = 1.8$ , which is a point located on one of  $\pi T$ -periodic lines on the stability diagram, see Fig. 8b, clearly these trajectories describe the linear resonance or instability caused by the forcing signal.

## 6 Conclusion

The present note covers the non-homogeneous Hill equation, this particular case presents new features in the stability diagram providing that the periodicity condition between the parametric and forcing signal is fulfilled, when this occurs, very thin curves (here called resonance lines) will appear inside the stable areas, such lines depict the linear resonance and emerge independently whether or not there is a commensurable relation between the forcing term and the parametric excitation signal. Then, it can be concluded that there are two types of instability associated with the forced Hill equation: the parametric resonance (well-known) and the linear resonance introduced in this paper.

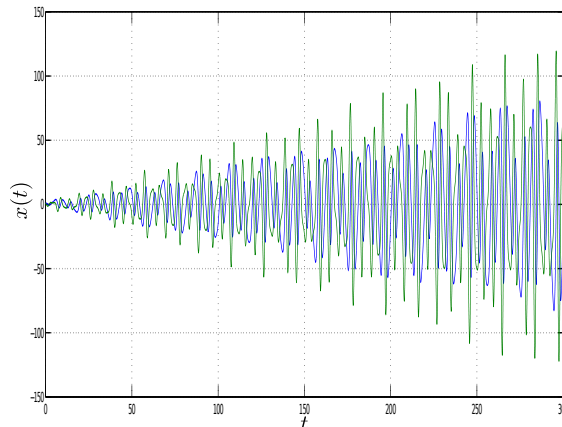


**Figure 9:** Response of the forced Kapitza pendulum:  $\ddot{x} + [\alpha + \beta \cos(t)]x = \cos(\pi t)$ ,  $\alpha = 2$  and  $\beta = 1.8$ .

This work also generalizes the results presented by Slane and Tragesser [8], about the inhomogeneous Hill equation, they described the changes operated only in the  $T$  and  $2T$  periodic solutions (the boundaries of the Arnold tongues).

Additionally, it was shown that the multipliers lying on the unit circle were shifted inside the circle when the damping effect was introduced in the non-homogeneous Hill equation. Consequently, the resonance lines disappeared.

A challenging problem appears when we try to characterize the periodic solutions and the resonance lines in the higher order Hill equation. Due to the fact that these systems experience a phenomena that does not occur in the two degree of freedom systems. Therefore, a greater effort is required.

## References

- [1] G.H. Hill. On the part of the motion of the lunar perigee which is a function of the mean motions of the sun and moon. *Acta Mathematica* **8** (1886) 1–36.
- [2] E. Mathieu. Memoire sur le Mouvement Vibratoire d'une Membrane de Forme Elliptique. *Journal de Mathématiques Pures et Appliquées* **13** (1868) 137–203.
- [3] J.W. Strutt. On the crispations of fluid resting upon a vibrating support. *Philosophical Magazine* **16** (1883) 50–58.
- [4] V. I. Arnol'd. Remarks on the perturbation theory for problems of Mathieu type. *Russian Math. Surveys* **38** (4) (1983) 215–233.
- [5] D. Shadman and B. Mehri. A non-homogeneous Hill's equation. *Applied Mathematics and Computation* **167** (2005) 68–75.
- [6] M.K. Kwong and J.S.W. Wong. On the oscillation of Hill's equation under periodic forcing. *Journal of Mathematical and Applications* **320** (2006) 37–55.
- [7] D. Younesian, E. Esmailzadeh and B. Sedaghati. Asymptotic solutions and stability analysis for generalized non-homogeneous Mathieu equation. *Communications in Nonlinear Science and Numerical Simulation*. **12** (2007) 58–71.

- [8] J. Slane and S. Tragesser. Analysis of Periodic Nonautonomous Inhomogeneous Systems. *Nonlinear Dynamics and Systems Theory* **11** (2) (2011) 183–198.
- [9] R. A. Ibrahim and A.D.S. Barr. Parametric vibration. Part 1: Mechanics of linear problems. *The Shock and Vibration Digest*. **10** (1978) 15–29.
- [10] A. Champneys. Dynamics of parametric excitation. *Math. of Comp. and Dyn. Sys.* (2011) 183–204.
- [11] C. Kaur, B. K. Sharma and S. Yadav. Resonance in the Motion of a Geo-Centric Satellite Due to the Poynting-Robertson Drag and Oblateness of the Earth. *Nonlinear Dynamics and Systems Theory* **19** (4) (2019) 497–511.
- [12] W. Magnus and S. Winkler. *Hill's Equation*. John Wiley & Sons, New York, 1966.
- [13] G.N. Jazar. Stability chart of parametric vibrating systems using energy-rate method. *International Journal of Non-Linear Mechanics* **39** (2004) 1319–1331.
- [14] K. Khachnaoui. Homoclinic Orbits for Damped Vibration Systems with Small Forcing Terms. *Nonlinear Dynamics and Systems Theory* **18** (1) (2018) 80–91.
- [15] V.A. Yakubovich and V.M. Starzhinskii. *Linear Differential Equations with Periodic Coefficients*. J. Wiley, New York, 1975.
- [16] R.W. Brockett. *Finite dimensional linear systems*. John Wiley and Sons, USA, 1970.
- [17] V. A. Yakubovich. Remark on a theorem of Floquet-Lyapunov. *Vestnik Leningrad Univ.* **25** (1970) 97–101.
- [18] K.R. Meyer, G.R. Hall and D. Offin. *Introduction to Hamiltonian Dynamical Systems and the N-Body Problem*. 2nd Ed., Springer, USA: Boston, 2009.
- [19] P. L. Kapitza. Dynamic stability of the pendulum with vibrating suspension point. *Sov. Phys. JETP*. **21**(5) (1951) 588–597.
- [20] E.I. Butikov. *Simulations of Oscillatory Systems*. CRC Press, New York, 2015.